ChemComm

Accepted Manuscript

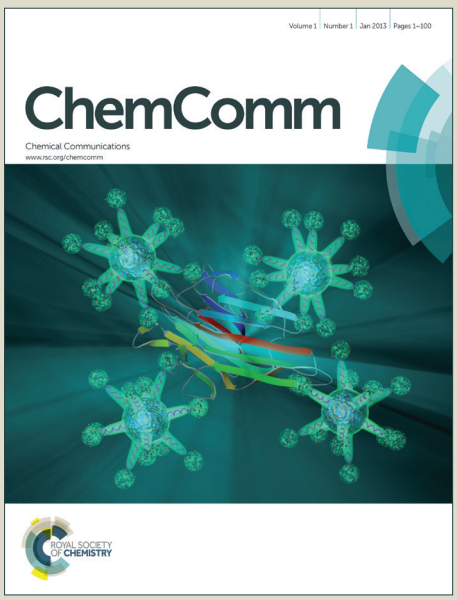

ROYAL SOCIETY OF CHEMISTRY

www.rsc.org/chemcomm

Cite this: DOI: 10.1039/c0xx00000x

www.rsc.org/xxxxxx

Communication

A fast-responsive mitochondria-targeted fluorescent probe detecting endogenous hypochlorite in living RAW 264.7 cells and nude mouse

Hongde Xiao[a], Kai Xin[b], Haifang Dou[a], Gui Yin[a,c*], Yiwu Quan[a], and Ruiyong Wang[b*]

Received (in XXX, XXX) Xth XXXXXXXXX 20XX, Accepted Xth XXXXXXXXX 20XX
DOI: 10.1039/b000000x

A very fast-responsive fluorescent probe PZ–Py for imaging mitochondrial HClO/ClO⁻, with a relatively long emission wavelength, was prepared. The limit of detection was evaluated to be 17.9 nM. Moreover, the probe PZ–Py was successfully applied in the imaging of endogenous HClO/ClO⁻ in mitochondria of RAW264.7 cells and living nude mouse.

Reactive oxygen species (ROS) have emerged as prevalent and important components of both physiological and pathological processes.[1] ROS are produced endogenously from oxygen. In this context, mitochondria are the major consumers of cellular oxygen and hence play a central role in ROS biology. The foremost function of mitochondria is to produce ATP, the major energy currency molecule of the cell. The process of producing ATP involves a series of electron–transport systems in the oxidation phosphorylation pathway, which is ascribed to be associated with the generation of reactive oxygen species (ROS).[2]

As a type of ROS, hypochlorous acid (HClO, pK_a 7.53) and its conjugate base hypochlorie (ClO^-) are widely employed as strong oxidizing agents in our daily life. In living organisms, the hypochlorite is produced mainly from hydrogen peroxide and chloride ions in a heme enzyme myeloperoxidase (MPO)–catalyzed reaction.[3] This is associated with innate host defence and is very important for killing a wide range of pathogens.[4] Thus, maintenance of appropriate level of HClO/ClO^- is fairly crucial for numerous cellular functions. However, abnormal overproduction of HClO/ClO^- is considered to be associated with some diseases, such as atherosclerosis, osteoarthritis, rheumatoid arthritis and even cancers.[5] Therefore, detecting mitochondrial HClO/ClO^- attracted extensive interests, especially taking advantages of fluorescent imaging techniques due to their high sensitivity, selectivity, rapid response rate and easiness of manipulating.[6]

[a]*State Key Laboratory of Analytical Chemistry for Life Science, School of Chemistry and Chemical Engineering, Nanjing University, Nanjing 210093, People's Republic of China. E-mail: yingui@nju.edu.cn*
[b]*State Key Laboratory of Pharmaceutical Biotechnology, School of Life Science, Nanjing University, Nanjing, 210093, China Email: wangry@nju.edu.cn*
[c]*Jiangsu Key Laboratory of Advanced Catalytic Materials and Technology, Changzhou University, 213164, China*

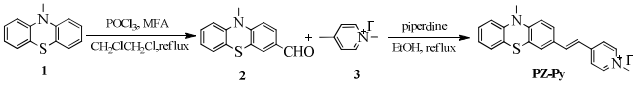

Scheme 1 Synthesis of the probe PZ–Py.

To date, a number of fluorescent probes detecting HClO/ClO^- have been developed,[7] and applied to the *in vitro* and *in vivo* imaging of HClO/ClO^-. However, those probes might encounter some problems, such as poor water solubility, interference from other ROS, low quantum yield, small Stokes Shift and relatively short emission wavelength. Meanwhile, only a very limited amount of mitochondria–targeted fluorescent probes have been reported.[8] And those fluorescent probes merely added a triphenylphosphonium (TPP) moiety or quaternized pyridine moiety, which have been utilized as mitochondria–targeted functional groups,[9] to the formerly reported probes.[10] Moreover, as far as biological applications were concerned, those mitochondria–targeted probes merely detected exogenous HClO/ClO^-, hence the mitochondrial target did not make any sense in this condition. Therefore, it is urgent to develop new effective mitochondria-targeted fluorescent probe for endogenous HClO/ClO^- with good water solubility, high sensitivity, fast response and excellent biocompatibility.

Herein, we reported an easily synthesized fluorescent probe PZ–Py based on phenothiazine and explored its fluorescent response to various ROS. Phenothiazine was chosen as the fluorogen due to its relatively longer emission wavelength, high quantum yield, large Stokes Shift, commercial available and good photo-stability. And the quaternized pyridine moiety was introduced as the mitochondria–targeted functional group, which also improve the compound's water solubility dramatically. The probe was prepared via a simple process (Scheme 1) and characterized using ^1H, ^{13}C NMR and HR–MS (see ESI).

First, we explored whether the probe PZ–Py could selectively detect HClO/ClO^- among the ROS including H_2O_2, $^{\cdot}OH$, O^{2-}, ^{t}BuOOH, NO, $ONOO^-$. To the solution of PZ–Py (5 μM) in PBS buffer (pH 7.3, 10 mM, containing 0.5% DMSO), various species of ROS were added respectively. As shown in Fig. 1, fluorescent signal of the solution of 5 μM PZ–Py in PBS buffer was very weak upon excitation at 400 nm. Addition of 50 μM ClO^- induced a great increase of fluorescence intensity at 562 nm. And the Stokes Shift was as large as 162 nm, which could diminish the influence of self-absorption to a great extent. Under excitation

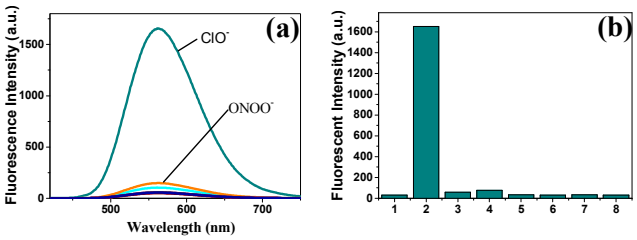

Fig. 1 (a) Fluorescence spectra and (b) fluorescence intensity of PZ–Py (5 μM) at 562 nm before and after addition of various ROS in PBS (pH 7.3, 10 mM, containing 0.5% DMSO). (1: blank, 2:ClO^-, 3:·OH, 4:$ONOO^-$, 5: O^{2-}, 6:^{t}BuOOH, 7: H_2O_2, 8:NO). [ClO^-]= 50 μM, [·OH] = [$ONOO^-$] = [O^{2-}] = [^{t}BuOOH] = [H_2O_2] = [NO] = 500 μM.

at 365 nm (hand-held UV lamp), strong yellow fluorescence could be observed upon the addition of ClO^- (inert of Fig. 2). However, other species of ROS (500 μM) caused negligible influence to the fluorescence of the probe. On the other hand, upon addition of ClO^-, colour of the solution changed from light brown to light yellow, accompanying the absorption peak blue-shifted from 438 nm to 407 nm (Fig. S1). And addition of other ROS had little effect on the absorption spectra. Considering the possible addition reactions of the α,β–unsaturated compounds with some nucleophiles, the fluorescence responses of PZ–Py towards different kinds of nucleophilic agents were tested. When 500 μM HSO_3^-, SCN^-, S^{2-}, CN^-, F^- or 1 mM GSH, Cys, Hcy was added into the solution of PZ–Py (5 μM) in PBS, as shown in Fig. S2, no obvious fluorescent enhancement could be detected. Therefore, PZ–Py was qualified to selectively detect ClO^- among the various competitive compounds.

Furthermore, to test the application extent of the PZ–Py as HClO/ClO^- probe, we next evaluated the fluorescent properties of the probe and its ability to react with HClO/ClO^- in a series of buffers with different pH values ranging from 4 to 10 (Fig. S3). In this pH range, responses of the probe to HClO/ClO^- were pH–independent, indicating that the assay is compatible with most biological applications, and the pH value of 7.3 was chosen for further fluorescent assay.

Then, the fluorescence titrations of the probe PZ–Py (5 μM) with HClO/ClO^- were conducted in PBS buffer (pH 7.3, 10 mM, containing 0.5% DMSO). As shown in Fig. 2, the fluorescence intensity at 562 nm increased gradually upon addition of ClO^-. At this point, a 40.5–fold fluorescent enhancement could be observed, accompanying the quantum yields increasing from 0.016 to 0.43. The fluorescence intensity remained changeless after the concentration of ClO^- was up to 80 μM (Fig. S4). The whole recognition process finished within just a few seconds and remained nearly changeless over time (Fig. S5). Such a short response time enabled the real-time detection of HClO. Moreover, a good linear relationship of emission intensity with the concentration of ClO^- could be obtained (Fig. S6), and the limit of detection (LOD=3σ/Slope) [11] towards HClO/ClO^- was evaluated to be 17.9 nM according to the linear fitting, demonstrating the very high sensitivity of PZ–Py to HClO/ClO^-.

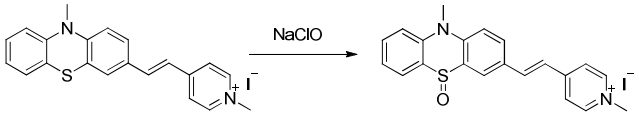

Scheme 2 The proposed reaction of PZ–Py with ClO^-.

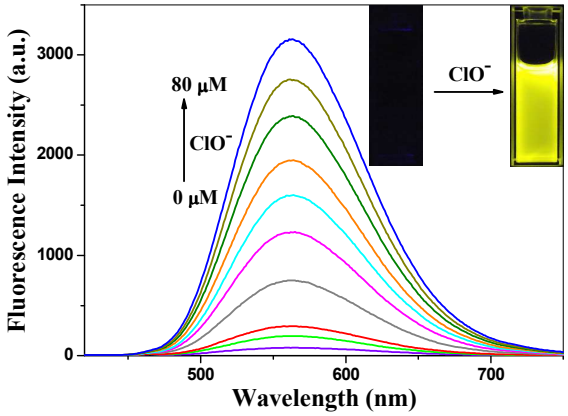

Fig. 2 Fluorescence titration spectra of PZ–Py (5 μM) upon addition of NaClO (0, 5, 10, 20, 30, 40, 50, 60, 70, 80 μM) in PBS (pH 7.3, 10 mM, containing 0.05% DMSO) upon excitation at 400 nm.

Moreover, we also conducted the absorption titration experiments. As shown in Fig. S7, the absorption peak of the probe at 441 nm decreased gradually as the addition of ClO^-, whereas another peak locating at 408 nm rose gradually. This blue shift of the peak corresponded to the colour change from light brown to light yellow (inert of Fig. S7). In the short–wavelength region a peak locating at 328 nm decreased gradually, symbolizing that the push-pull electronic conjugate structure has changed.

In organic reactions, thioether could be oxidized to sulfoxide or sulfone by specific oxidant. Thus, we assumed that the divalent sulphur of our probe was oxidized by NaClO and then the fluorescence was turned on. To verify the assumed detection mechanism of PZ–Py towards HClO/ClO^-, the product of PZ–Py reacted with HClO/ClO^- was purified over silica gel column as the pure product. Then, the HR–MS and ^{13}C NMR data (Fig. S8 & Fig. 9) confirmed that the mechanism was oxidation of the divalent sulphur to sulfoxide rather than cleavage of the carbon–carbon double bond like some reported probes with strong electron-withdrawing groups linked by carbon–carbon double bond, [12] and we proposed the possible mechanism of PZ–Py detecting HClO/ClO^- as depicted in Scheme 2. Moreover, ^{1}H NMR (Fig. S10) showed two hydrogen atoms of the carbon–carbon double bond, eliminating the possibility of epoxidation of the carbon–carbon double bond to generate the product shown in Fig. S11.

The desirable fluorescence properties of PZ–Py for HClO/ClO^- prompted us to utilize it for the detection of intracellular HClO/ClO^-. We first explored whether PZ–Py could detect exogenous HClO/ClO^- in HeLa cells (Fig. 3). As shown in Fig.3.a, the living HeLa cells were incubated with PZ–Py (5 μM) in culture medium for 10 min, and exhibited no fluorescence. After treated with NaClO (20 μM) for 15 min, intense yellow fluorescence emerged in the cells (Fig.3.c). The merged picture, as shown in Fig.3.d, confirmed that the fluorescence signals are only located in the intracellular area. The above experiments proved that the probe PZ–Py was well cell–permeated and able to detect exogenous HClO/ClO^- in living HeLa cells.

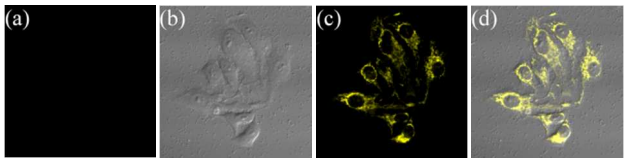

Fig. 3 Confocal fluorescence images of HeLa cells (λ_{ex}=405 nm, λ_{em}: 530–630 nm). (a) Fluorescent image of HeLa cells stained with probe PZ–Py (5 μM) for 10 min. (b–d) HeLa cells were then incubated with NaClO (20 μM) for another 15 min. (b) bright field image; (c) fluorescent image; and (d) merged image.

We then investigated whether the probe PZ–Py was capable of detecting intracellular endogenous HClO/ClO^-. When stimulated by lipopolysaccharide (LPS) and phorbol myristate acetate (PMA), macrophages may produce endogenous HOCl.[13] MTT assay revealed that cell viability was rarely changed when 5 μM PZ–Py was added for 24 h (Fig. S12). In the control group, the living RAW264.7 macrophage cells were incubated with PZ–Py (5 μM) in culture medium for 10 min at 37 ℃, and exhibited no fluorescence (Fig.4.a). Whereas in the experiment group, after the macrophage cells have been incubated with LPS (1 μg/mL) for 5 h, and then further coincubated with PMA (1μg/mL) and PZ–Py (5 μM) for 10 min, obvious yellow fluorescence could be detected in the cells (Fig.4.c). And the merged picture confirmed that the fluorescence signals are only located in the intracellular area. The aforementioned phenomena showed that PZ–Py was well cell–permeated and capable of imaging endogenous HClO in the living RAW264.7 macrophage cells.

To further examine the sub-cellular localization of PZ–Py, Mito Tracker green, a widely used commercially available mitochondrial dye, was employed for a co–localization study (Fig. 5). As depicted in Fig.5.e, the changes in the intensity profiles of linear regions of interest (ROIs) (the probe PZ–Py and Mito Tracker Green co–staining) were synchronous, the fluorescent signals of PZ–Py responded to HClO overlaid well with the fluorescence of Mito Tracker Green. Moreover, co-localization was qualified using Pearson's sample correlation factors (Rr). The intensity of correlation plot (Fig.5.f) revealed a high Pearson's coefficient (0.96), confirming that PZ–Py was specifically located in the mitochondria of the living RAW264.7 macrophage cells. Furthermore, co–localization study employing HeLa cells (Fig. S13, Rr=0.93) also showed that the probe could be mitochondria–targeted in living HeLa cells.

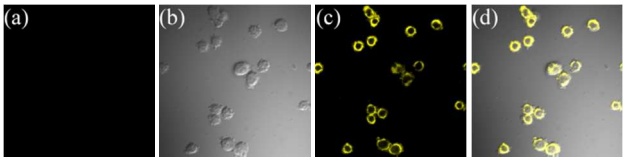

Fig. 4 Confocal fluorescence images of RAW 264.7 cells (λ_{ex}=405 nm, λ_{em}: 530–630 nm). (a) Fluorescent image of RAW 264.7 cells stained with probe PZ–Py (5 μM) for 10 min. (b–d) RAW 264.7 cells were incubated with LPS (1 μg/mL) for 5 h, further incubated with PMA (1 μg/mL) and PZ–Py (5 μM) for 20 min. (b) bright field image; (c) fluorescent image; and (d) merged image.

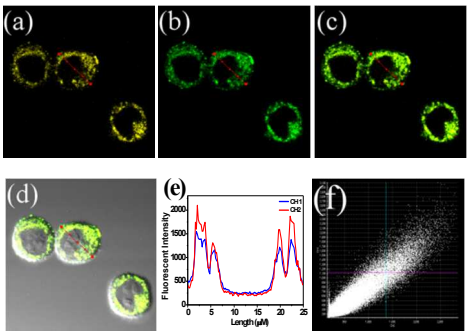

Fig. 5 (a–d) Confocal fluorescence images of RAW 264.7 cells. The cells were incubated with LPS (1 μg/mL) for 5 h, further incubated with PMA (1 μg/mL), PZ–Py (5 μM), and Mito Tracker Green (100 nM) for 20 min. (a) emission from the yellow channel, λ_{ex}=405 nm, λ_{em}: 531–590 nm; (b) emission from the green channel (mitochondrial staining, λ_{ex}=488 nm, λ_{em}: 500–530 nm); (c) merged image of a and b; (d) merged image of c and bright–field image. (e) Intensity profile of ROIs across RAW 264.7 cells. Red lines represent the intensity of the probe PZ–Py and blue lines represent the intensity of Mito Tracker Green. (f) Correlation plot of Mito Tracker Green and PZ–Py intensities.

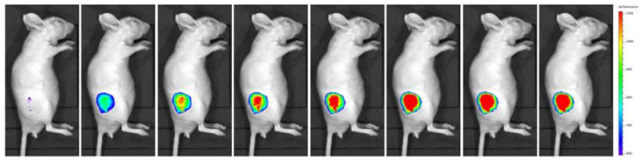

Fig. 6 Representative fluorescence images (pseudocolor) of a nude mouse. The mouse was given a skin-pop injection of LPS (100 μL×1 μg/mL) for 12 h, then a injection of PMA (50 μL×1 μg/mL) for 30 min, finally a skin-pop injection of PZ–Py (50 μL×50 μM). Images were taken after incubation for 0, 5, 10, 15, 20, 30, 45 and 60 min, respectively. Images were taken using an excitation laser of 430 nm and an emission filter of DsRed channel.

We then evaluated the suitability of the probe for imaging endogenous HClO in living animals. The HClO produced *in vivo* was generated by activated macrophages and neutrophils in a lipopolysaccharide (LPS) model of acute inflammation.[14]

In this case, nude mice were selected as our model. In the experiment group (Fig. 6), a solution of LPS (100 μL×1 μg/mL) was injected into the back of the mouse, and 12 hours later, PMA (50 μL×1 μg/mL) was then injected into the same region. After 30 min of the above disposal, the probe (50 μL×20 μM in saline, containing 1% DMSO) was injected into the same region. On the other hand, the control group (Fig. S14) was treated likewise, except substituting saline for LPS or PMA. The pictures were taken under the imaging system after the mouse was treated for 0, 5, 10, 15, 20, 30, 45 and 60 min, respectively. As shown in Fig. S14, no fluorescent intensity could be detected in the back of the mouse, whereas the fluorescence signals of the experiment group became stronger and stronger gradually within 30 min and then remained changeless. The result established that PZ–Py was a desired probe for imaging endogenous HClO *in vivo*.

In summary, a sensitive fluorescent probes PZ–Py for ClO^- was developed and exhibited excellent selectivity towards ClO^- over other ROS with high sensitivity. Detections of intracellular HClO were conducted employing living RAW264.7 macrophage cells. The probe could target on mitochondria successfully taking advantage of the pyridine unit. Finally, the probe was applied in the *in vivo* detection of endogenous HClO using living mice.

This work was supported by the National Natural Science Foundation of China (No. 21174061), National Basic Research Program of China (No. 2014CB846004), Jiangsu Key Laboratory of Advanced Catalytic Materials and Technology (No. BM2012110) and Jiangsu Province Science Technology Innovation and Achievements Transformation Special Fund (BY2012149).

Notes and references

1 (*a*) J. R. Stone and S. Yang, *Antioxid Redox Sign*, 2006, **8**, 243; (*b*) B. DAutrEaux and M. B. Toledano, *Nat. Rev. Mol. Cell Biol.*, 2007, **8**, 813; (*c*) C. C. Winterbourn, *Nat. Chem. Biol.*, 2008, **4**, 278; (*d*) G. C. Bittner, C. R. Bertozzi, and C. J. Chang, *J. Am. Chem. Soc.*, 2013, **135**, 1783.

2 (*a*) A. T. Hoye, J. E. Davoren, P. Wipf, M. P. Fink, V. E. Kagan, *Acc. Chem. Res.*, 2008, **41**, 87; (*b*) C. W. T. Leung, Y. N. Hong, S. J. Chen, E. G. Zhao, J. W. Y. Lam and B. Z. Tang, *J. Am. Chem. Soc.*, 2013, **135**, 62.

3 (*a*) J. E. Harrison and J. Schultz, *J. Biol. Chem.*, 1976, **251**, 1371; (*b*) Y. W. Yap, M. Whiteman and N. S. Cheung, *Cell. Signalling*, 2007, **19**, 219.

4 Z. M. Prokopowicz, F. Arce, R. Biedron, C. L. L. Chiang, M. Ciszek, D. R. Katz, M. Nowakowska, S. Zapotoczny, J. Marcinkiewicz and B. M. Chain, *J. Immunol.*, 2010, **184**, 824.

5 (*a*) A. Daugherty, J. L. Dunn, D. L. Rateri and J. W. Heinecke, *J. Clin. Invest.*, 1994, **94**, 437; (*b*) S. M. Wu and S. V. Pizzo, *Arch. Biochem. Biophys.*, 2001, **391**, 119; (*c*) S. Weitzman and L. Gordon, *Blood*, 1990, **76**, 655.

6 (*a*) H. D. Xiao, K. Chen, N. N. Jiang, D. D. Cui, G. Yin, J. Wang, R. Y. Wang, *Analyst*, 2014, **139**, 1980; (*b*) B. C. Dickinson, V. S. Lin, C. J. Chang, *Nat. Protoc.*, 2013, **8**, 1249; (*c*) R. Azadbakht and J. Khanabadi, *Inorg. Chem.Comm.*, 2013, **30**, 21.

7 (*a*) S. Kenmoku, Y. Urano, H. Kojima and T. Nagano, *J. Am. Chem. Soc.*, 2007, **129**, 7313; (*b*) X. Chen, X. Wang, S. Wang, W. Shi, K. Wang and H. Ma, *Chem.–Eur. J.*, 2008, **14**, 4719; (*c*) Y. K. Yang, H. J. Cho, J. Lee, I. Shin and J. Tae, *Org. Lett.*, 2009, **11**, 859; (*d*) G. Chen, F. Song, J. Wang, Z. Yang, S. Sun, J. Fan, X. Qiang, X. Wang, B. Dou and X. J. Peng, *Chem. Commun.*, 2012, **48**, 2949; (*e*) Q. Xu, K.–A. Lee, S. Lee, K. M. Lee, W. J. Lee and J. Yoon, *J. Am. Chem. Soc.*, 2013, **135**, 9944.

8 (*a*) G. H. Cheng, J. L. Fan, W. Sun, K. Sui, X. Jin, J. Y. Wang and X. J. Peng, *Analyst*, 2013, **138**, 6091; (*b*) J. T. Hou, M. Y. Wu, K. Li, J. Yang, K. K. Yu, Y. M. Xie and Xi. Q. Yu, *Chem. Commun*., 2014, **50**, 8640.

9 (*a*) A. T. Hoye, J. E. Davoren and P. Wipf, *Acc. Chem. Res.*, 2008, **41**, 87; (*b*) E. M. Nolan, J. W. Ryu, J. Jaworski, R. P. Feazell, M. Sheng and S. J. Lippard, *J. Am. Chem. Soc.*, 2006, **128**, 15517; (*c*) S. C. Dodani, S. C. Leary, P. A. Cobine, D. R. Winge and C. J. Chang, *J. Am. Chem. Soc.*, 2011,**133**, 8606.

10 (*a*) M. Emrullahoglu, M. Uçuncu and E. Karakus, *Chem. Commun.*, 2013, **49**, 7836; (*b*) X. Q. Chen, X. C. Wang, S. J. Wang, W. Shi, K. Wang and H. M. Ma, *Chem. – Eur. J.*, 2008, **14**, 4719.

11 (*a*) K. Tsukamoto, Y. Shinohara, S. Iwasaki, H. Maeda, *Chem. Commun.*, 2011, **47**, 5073; (*b*) J. Y. Kim, J. Park, H. Lee, Y. Choi, Y. M. Kim, *Chem. Commun.*, 2014, **50**, 9353; (*c*) B. S. Wang, P. Li, F. B. Yu, J. S. Chen, Z. J. Qu, K. L. Han, *Chem. Commun.*, 2013, **49**, 5790.

12 (*a*) F. Liu, T. Wu, J. F. Cao, H. Zhang, M. M. Hu, S. G. Sun, F. L. Song, J. L. Fan, J. Y. Wang, X. J. Peng, *Analyst*, 2013, **138**, 775; (*b*) J. Park, H. J. Kim, Y. D. Choi and Y. M. Kim, *Analyst*, 2013, **138**, 3368.

13 Y. Adachi, A. L. Kindzelskii, A. R. Petty, J. B. Huang, N. Maeda, S. Yotsumoto, Y. Aratani, N. Ohno, H. R. Petty, *J. Immunol.*, 2006, **176**, 5033.

14 K. Kundu, F. Knight, N. Willett, S. Lee, W. R. Taylor, N. Murthy, *Angew. Chem. Int. Ed.*, 2009, **48**, 299.